Program for the interpretive optimization of two-dimensional resolution

Pirok, B.W.J.; Pous-Torres, S.; Ortiz-Bolsico, C.; Vivó-Truyols, G.; Schoenmakers, P.J.

DOI
10.1016/j.chroma.2016.04.061

Publication date
2016

Document Version
Final published version

Published in
Journal of Chromatography A

Journal of Chromatography A, 1450 (2016) 29–37

Contents lists available at ScienceDirect

Journal of Chromatography A

journal homepage: www.elsevier.com/locate/chroma

Program for the interpretive optimization of two-dimensional resolution☆

Bob W.J. Pirok[a,b,*], Sandra Pous-Torres[a,c], Cassandra Ortiz-Bolsico[a,c], Gabriel Vivó-Truyols[a], Peter J. Schoenmakers[a]

[a] University of Amsterdam, van't Hoff Institute for Molecular Sciences, Analytical-Chemistry Group, Science Park 904, 1098 XH Amsterdam, The Netherlands
[b] TI-COAST, Science Park 904, 1098 XH Amsterdam, The Netherlands
[c] Departament de Química Analítica, Universitat de València, c/Dr. Moliner 50, Burjassot 46100, Spain

ARTICLE INFO

Article history:
Received 17 February 2016
Received in revised form 20 April 2016
Accepted 21 April 2016
Available online 29 April 2016

Keywords:
Pareto-optimality
interpretive optimization
LC × LC
method development
synthetic dyes
retention prediction

ABSTRACT

The challenge of fully optimizing LC × LC separations is horrendous. Yet, it is essential to address this challenge if sophisticated LC × LC instruments are to be utilized to their full potential in an efficient manner. Currently, lengthy method development is a major obstacle to the proliferation of the technique, especially in industry. A program was developed for the rigorous optimization of LC × LC separations, using gradient-elution in both dimensions. The program establishes two linear retention models (one for each dimension) based on just two LC × LC experiments. It predicts LC × LC chromatograms using a simple van-Deemter model to generalize band-broadening. Various objectives (analysis time, resolution, orthogonality) can be implemented in a Pareto-optimization framework to establish the optimal conditions. The program was successfully applied to a separation of a complex mixture of 54 aged, authentic synthetic dyestuffs, separated by ion-exchange chromatography and ion pair chromatography. The main limitation experienced was the retention-time stability in the first (ion-exchange) dimension. Using the PIOTR program LC × LC method development can be greatly accelerated, typically from a few months to a few days.

1. Introduction

During the last decade, comprehensive two-dimensional liquid chromatography (LC × LC) has matured into a highly valuable tool for the analysis of complex mixtures. For example, LC × LC was successfully applied for the characterization of phospholipids [1], proteins and peptides [2,3], procyanidins [4] and antibodies [5]. For the detailed characterization of complex polymers with more than one chemical distribution, LC × LC is virtually indispensable [6]. The success of the technique is based on the increased peak capacity in comparison with one-dimensional LC and on the additional selectivity obtained from different separation mechanisms in the two dimensions.

However, method development in LC × LC is considerably more complex than in one-dimensional LC. With the advent of state-of-the-art instrumentation for LC × LC, the number of options to realize and optimize LC × LC separations has increased dramatically. For example, contemporary LC × LC systems support different gradient-elution programs in each individual second-dimension run. This provides an extraordinary range of possibilities for solving separation problems. However, the challenge of fully optimizing LC × LC separations becomes daunting. Yet, this challenge must be overcome if sophisticated LC × LC instruments are to be utilized efficiently and to their full potential.

A complete LC × LC method requires not only a decision on two orthogonal mechanisms and a number of sample-independent physical parameters (*e.g.* column dimensions, particle sizes, flow rates, modulation time), but it also involves an optimal choice of a number of chemical parameters that affect the selectivity. This typically concerns the mobile-phase composition as a function of time, possibly augmented by changes in other parameters, such as temperature, pH or buffer strength. A comprehensive optimization involves all sample-independent (physical) parameters and an intricate tailoring of the parameters that affect retention and selectivity. Impressive LC × LC applications have been achieved thanks to the knowledge and expertise of the respective analysts [1–5],

☆ Selected paper from 14th International Symposium on Hyphenated Techniques in Chromatography and Separation Technology, 27–29 January 2016, Ghent, Belgium.

* Corresponding author.
E-mail address: B.W.J.Pirok@uva.nl (B.W.J. Pirok).

http://dx.doi.org/10.1016/j.chroma.2016.04.061
0021-9673/

but usually through lengthy method-development processes. The expertise and time required render the development of industrial LC × LC applications extremely costly, which impairs the proliferation of the technique.

A number of studies have been devoted to strategies for optimizing various aspects of LC × LC methods. Dugo et al. minimized peak disturbances resulting from mobile-phase immiscibility problems for normal-phase and reversed-phase liquid chromatography LC × LC separation systems [7]. The coupling of these two separation mechanisms is notorious for giving rise to distorted or split peaks, due to immiscibility of the respective mobile phases. Gu et al. [8] investigated the optimization of the peak capacity through the column length, flow rate and eluent composition by using Poppe's approach [9]. Kalili et al. optimized a hydrophilic-interaction liquid chromatography × reversed-phase liquid chromatography separation system and compared on-line, off-line and stop-flow LC × LC modes [10]. In their work, the authors took into account effects of under-sampling of the first-dimension chromatogram, the degree of orthogonality, and additional band broadening induced by stop-flow analysis. For optimization the authors used the peak capacities of individual one-dimensional experiments obtained at different gradient times for all three configurations, relating the total peak capacity with the total analysis time. Česla et al. developed a method to optimize segmented gradient profiles in the two dimensions [11]. The resulting optimization approach allowed the LC × LC separation time to be reduced from 700 to 30 min.

All these studies contribute to our understanding of LC × LC separations and to the realization of useful LC × LC tools, but they have not resulted in a faster or easier method-development process. The development of LC × LC methods is still knowledge intensive and time consuming [7,8,10,11]. Our group seeks to develop algorithms and software that allow liquid chromatographers to greatly reduce the time needed to develop LC × LC methods and to benefit fully from the great advantages of this technique. We have developed a Pareto-optimality approach to comprehensively optimize all physical parameters [12]. A more challenging step is to rigorously optimize all chemical parameters that affect retention and selectivity, such as the mobile-phase composition, temperature, pH and buffer strength. In the present work, we demonstrate the feasibility of optimizing first-dimension gradients and second-dimension gradient assemblies (*e.g.* shifting gradients) in LC × LC separations for a specific sample, interpretively, based on a very small number of experiments, modelling of the retention, and generalizing band-broadening behaviour of individual sample components. Gradients of different form (linear or curved) and different complexity (one or more segments) can be used. We will restrict ourselves to the simplest form (single segment linear gradients), which are commonly used to address the majority of LC separation problems. We describe algorithms to predict retention for all possible simulated gradient combinations and an interactive Pareto-optimality approach to locate a suitable optimum. We apply this approach to the separation of a complex mixture of degraded synthetic dyes by ion-exchange chromatography × ion-pair reversed-phase chromatography.

2. Theory

Comprehensive two-dimensional liquid chromatography requires optimizing two one-dimensional separations. The retention behaviour of a solute in isocratic reversed-phase liquid chromatography (RPLC) can be approximately described by a linear relationship between the logarithm of the retention factor (k) and the volume fraction of strong solvent (φ)

$$\ln k = \ln k_0 - S\varphi \tag{1}$$

Here, k_0 depicts the extrapolated retention factor of the analyte when φ equals 0 (*i.e.* pure water), and S the change in retention factor with increasing mobile phase strength. Two experimental retention times suffice for determining k_0 and S. Once these values are known, the retention factor can be predicted for any φ. The values of k_0 and S can also be determined from gradient-elution RPLC experiments. For linear gradients in RPLC, the retention time can be calculated from [13]

$$t_{R,gradient} = \frac{1}{SB}\ln\left\{1 + SBk(A)\left[t_0 - \frac{t_{init} + t_D}{k(A)}\right]\right\} + t_0 + t_D + t_{init} \tag{2}$$

Here, A represents φ at the start of the gradient, B the change in φ as a function of time (*i.e.* the slope of the gradient), t_0 the column dead time, t_D the dwell time of the system and t_{init} the time before the gradient is programmed to start. Provided that S and $k(A)$ (and thus k_0) are known for a solute, and that the reversed-phase model (Eq. (1)) is valid, the retention times can be predicted for any gradient. To establish $\ln k_0$ and S, retention data are required from a minimum of two sufficiently different gradients. If the gradient slopes differ by a factor of at least three [14,15], accurate values for S and $\ln k_0$ can be found by solving the two equations for two unknowns. Interestingly, this approach can simultaneously be applied to all compounds for which the retention times can be established in two one-dimensional separations. The principle can also be utilized simultaneously in two dimensions if (approximate) retention models for each dimension are known for all analytes for which two retention times under different conditions can be unequivocally determined. To meet the latter condition, it suffices to pinpoint corresponding peaks in the two 2D chromatograms; the identity of the peak does not need to be established. Thus, in principle, only two two-dimensional chromatograms are required to predict retention under any gradient conditions in both dimensions.

The previously developed method for the separation of synthetic dyestuffs utilized an isocratic section preceding and following the gradient in the first dimension [16]. It is important that the algorithm is able to take these situations into account for both RPLC and IEC.

2.1. Reversed-phase chromatography

Schoenmakers et al. developed a model for RPLC which accounted for components eluting before, during and after the gradient [13]. In the event that the component elutes before the gradient its retention time is given by

$$t_{R,before} = t_0(1 + k(A)) \tag{3}$$

If $t_{R,before} > t_0 + t_D + t_{init}$ then either the component experiences the gradient and the algorithm will calculate the retention time $t_{R,gradient}$ of the component according to Eq. (2), or if, $t_{R,gradient} > t_0 + t_D + t_{init} + t_G$, where t_G is the total gradient time, the component elutes after the end of the gradient and its retention is calculated as

$$t_{R,after} = k_f\left(t_0 - \frac{t_D + t_{init}}{k(A)}\right) - \frac{1}{B\ln k_0}\left(1 - \frac{k_f}{k(A)}\right) + t_G + t_D + t_{init} + t_0 \tag{4}$$

Here, k_f depicts the retention factor at the end of the gradient.

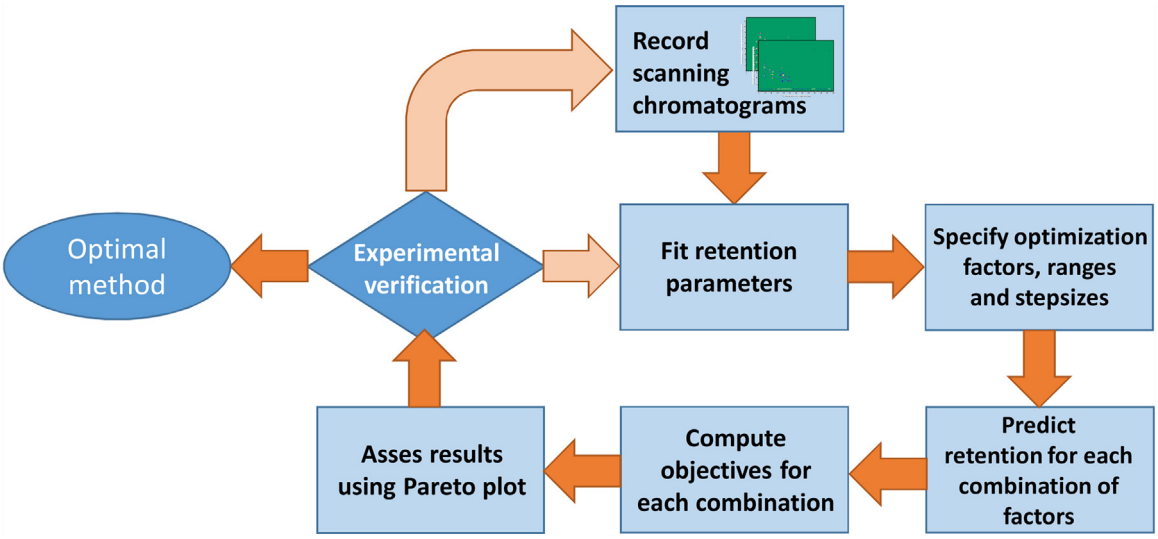

Fig. 1. Flowchart depicting the main steps of the PIOTR program for optimization of an LC × LC method. Application starts at the top, after two scanning experiments have been performed. During experimental verification it may be concluded that the re4tention models may be improved using the additional data (possibly using a non-linear model). Also, more peaks may be detected in the optimized chromatogram than in the scanning runs. In that case the new chromatogram serves as one of two new scanning runs. A second (significantly slower or faster) experiment will then be needed. When the experimental chromatogram is satisfactory the optimization is finished.

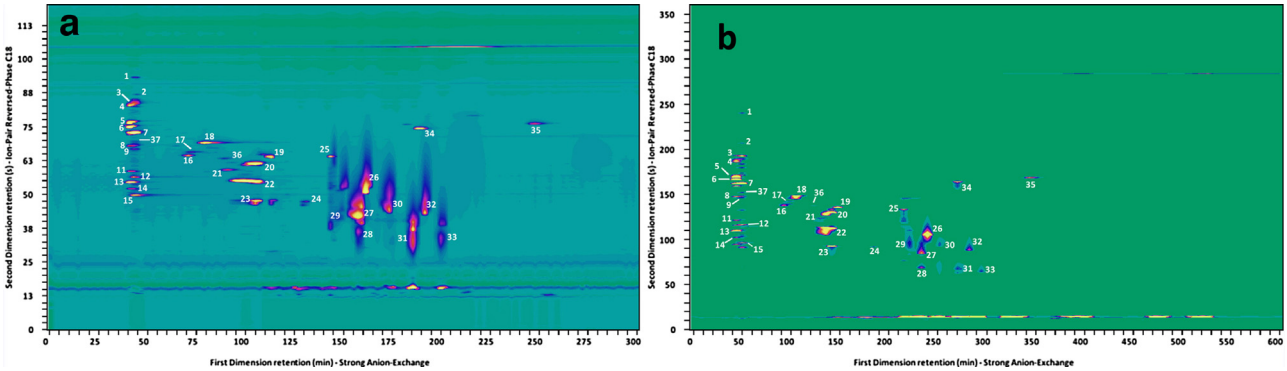

Fig. 2. LC × LC-UV chromatograms of the separation of a mixture of 54 synthetic dyes using steep and shallow gradients according to methods described in the Experimental section. Chromatogram a represents the separation using fast gradients of 180 and 1.5 minutes in the first and second dimensions, respectively, whereas chromatogram b displays the separation using slow gradients of 540 and 4.5 minutes. Retention times for identically annotated peaks were paired to determine retention parameters.

2.2. Ion-Exchange Chromatography

In isocratic ion-exchange chromatography, the buffer concentration is kept constant and the retention factor of a compound can be described as [17]

$$\ln k = \ln k_0 - n \ln [c] \tag{5}$$

Here, n is related to the charge of the component and $[c]$ represents the buffer concentration. Jandera et al. described the gradient elution model for ion-exchange chromatography taking into account the elution of a component in an isocratic section before the gradient and during the gradient itself [17]. In this work, we have expanded this set of equations to account for the event of a component eluting after the gradient. Similar to RPLC, the algorithm will use Eq. (3) in the event that the component elutes before the start of the gradient. However, in this case, Eq. (5) is used to calculate k(A). If $t_{R,before} > t_0 + t_D + t_{\text{init}}$ is true, then the component is overtaken by the gradient and its retention will be provided by

$$t_{R,gradient} = \frac{\left[k_0 \left(t_0 - \frac{t_{\text{init}} + t_D}{k(A)}\right) B(n+1) + c_{\text{init}}^{n+1}\right]^{\frac{1}{n+1}}}{B} - \frac{c_{\text{init}}}{B} + t_0 + t_{\text{init}} + t_D \tag{6}$$

where c_{init} is the initial buffer concentration at the start of the gradient, B is (as before) the slope of the gradient, and k(A) is the retention factor at the beginning of the gradient. In the event that the component elutes after the gradient ($t_{R,gradient} > t_0 + t_D + t_{\text{init}} + t_G$) its retention time is described by

$$t_{R,after} = k_{\text{final}} \left(t_0 - \frac{t_{\text{init}} + t_D}{k_{\text{init}}}\right) - \frac{k_{\text{final}}}{Bk_0(n+1)} \left[c_{\text{final}}^{n+1} - c_{\text{init}}^{n+1}\right] + t_0 + t_{\text{init}} + t_D + t_G \tag{7}$$

where c_{final} is the buffer concentration at the end of the gradient.

3. Experimental

3.1. Instrumental

All experiments were carried out on an Agilent 1290 Infinity 2D-LC system equipped with two binary pumps (G4220A; one for each dimension), a diode-array detector (G4212A) with an Agilent Max-Light Cartridge Cell (G4212-6008, 10 mm, V_{det} = 1.0 μL), an autosampler (G4226A), two thermostatted column compartments (G1316C), of which the compartment for the second dimension was equipped with a 2-position 8-port valve (G4236A) in which two calibrated 60-μL loops were installed. In front of the first-dimension

column, an Agilent 1290 Infinity In-Line Filter (G5067-4638) was installed to protect the column. The dwell volumes for the first and second dimensions were approximately 196 μL and 73 μL, respectively. The injector needle was set to draw and eject at a speed of 10 μL/min with two seconds equilibration time. The flow rates were 10 μL/min in the first dimension and 2.4 mL/min in the second dimension.

For the comprehensive separation of the synthetic dyestuffs by LC × LC, two columns were used. In the first dimension, an Agilent PL-SAX 150 × 2.1 mm i.d.; 8-μm particle diameter (PL1951-3802) column was installed. In the second dimension, an Agilent ZORBAX Eclipse Plus RRHT 50 × 4.6 mm; 1.8 μm (959941-902) column was used. The chromatographic system was controlled using Agilent OpenLAB CDS Chemstation Edition (Rev. C.01.04 [35]) software.

The program, its Graphical User Interface (GUI) and all algorithms were written in-house in a

MATLAB 2015a (Mathworks, Woodshole, MA, USA) environment (see Supplementary material Fig. S1 for screenshots of the GUI windows).

3.2. Chemicals

Aqueous solutions were prepared using deionised water (Arium 611UV, Sartorius, $R = 18.2\ M\Omega\ cm$, Germany). Methanol (ULC/MS grade) was obtained from Biosolve (Valkenswaard, The Netherlands). Acetonitrile (ACN, LC–MS grade) was obtained from Avantor Performance Chemicals (Deventer, The Netherlands). Ammonium sulphate (BioXtra, ≥99%), formic acid (reagent grade, ≥95%) and tetramethylammonium-hydroxide solution (TMA, 25% in water) were obtained from Sigma-Aldrich (Darmstadt, Germany). 54 samples of authentic dyestuff from the period 1850 to 1920 were obtained from to the reference collection of the Cultural Heritage Agency of the Netherlands (RCE, Amsterdam, The Netherlands).

3.3. Analytical Conditions

3.3.1. Sample preparation

For each dyestuff a 5000 ppm solution by weight was prepared in water/methanol 1:1 (v/v) after which 100 μL of each dyestuff solution was aliquoted into one vial to result in a mixture where each dyestuff was at a concentration of approximately 100 ppm.

3.3.2. Methods

The initial methods used in this study were adapted from earlier published work [16]. The following section describes the exact gradients programmed for each experiment presented in this study.

In the first dimension, the mobile phase comprised water/acetonitrile 1:1 [v/v] (Mobile Phase A), and 100 mM ammonium sulphate in water/acetonitrile [v/v] 1:1 (Mobile Phase B). Both mobile phase A and B were brought to pH 7.5 using TRIS buffer. In the second dimension, the used mobile phase was 10 mM tetramethylammonium hydroxide in water/acetonitrile 95:5 [v/v], brought to pH 3.0 with formic acid as mobile phase A and acetonitrile/water 95:5 [v/v] as mobile phase B.

For the fast scanning experiment, a modulation time of 2 minutes was used. The first-dimension gradient program was: 0–10 min isocratic at 100% A; 10–190 min, linear gradient to 100% B; 190–200 min, linear gradient to 100% A; maintained at 100% A for 40 min. The second dimension gradient program was: 0–1.5 min, linear gradient from 100% A to 100% B; 1.5–1.6 min, linear gradient to 100% A; maintained at 100% A for 0.4 min, until the next modulation.

For the slow scanning experiment, a modulation time of 6 min was employed, with ^1D gradient program: 0–10 min isocratic at 100% A; 10–550 min, linear gradient to 100% B; 550 to 560 min, linear gradient to 100% A; maintained at 100% A for 40 min. ^2D gradient program: 0–4.5 min, linear gradient from 100% A to 100% B; 4.5–4.6 min, linear gradient to 100% A; maintained at 100% A for 1.4 min, until the next modulation.

For the interpolation experiment, a modulation time of 4 minutes was employed, with ^1D gradient program: 0 to 10 min isocratic at 100% A; 10–370 min, linear gradient to 100% B; 380 to 390 min, linear gradient to 100% A; maintained at 100% A for 60 min. ^2D gradient program: 0–3.0 min, linear gradient from 100% A to 100% B; 3.0–3.1 min, linear gradient to 100% A; maintained at 100% A for 0.9 min, until the next modulation.

For the predicted Pareto-optimal experiment, a modulation time of 2 minutes was employed, with ^1D gradient program: 0–10 min isocratic at 100% A; 10–80 min, linear gradient to 100% B; 80 to 90 min, linear gradient to 100% A; maintained at 100% A for 150 min. ^2D gradient program: 0–1.5 min, linear gradient from 20% B to 100% B; 1.5–1.6 min, linear gradient to 20% B; maintained at 20% B for 0.4 min, until the next modulation.

4. Results and Discussion

4.1. Input Data

Fig. 1 shows a schematic summary of the PIOTR program. The first action is shown at the top. Source chromatograms are interpreted by fitting the retention parameters for all compounds. To fit the retention parameters accurately, the program requires the retention times of the compounds of interest in both dimensions from two scanning LC × LC experiments (*i.e.* the peak table of one slow and one fast experiment), where the gradient slopes in both dimensions of one experiment differ by at least a factor of three relative to the other experiment. As the purpose of these scanning experiments is to fit the retention factors of as many compounds as possible, it is advisable to use gradients that cover a broad range (*e.g.* 5–100% of organic modifier in RPLC). The two 2D chromatograms obtained from the two scanning experiments used in this study are shown in Fig. 2. Of course, the location of a peak relative to its location in the other experiment needs to be determined, so that the retention times of the same compound peak are obtained from both experiments (see Supplementary materials Table S1 for the peak tables of these two experiments). Cross assignments between the two input chromatograms were based on the relative intensities of peaks, and on relative retention times, and UV spectra of each peak. Usually, cross assignments do not require meticulous efforts for every single peak. Often clearly identifiable peak patterns can be discerned in the two input chromatograms. For complex samples, cross assigning peaks between two LC × LC chromatograms becomes significantly more difficult. The use of MS or UV-spectra is then extremely helpful.

In order to use the retention times to fit the retention parameters of each compound, the conditions under which the retention times were obtained (*e.g.* gradient times, flow rates, *etc.*) and a number of system properties must be known to the program, such as the dead and dwell volumes of both dimensions (V_0 and V_D, related to t_0 and t_D by the flow rate), the modulation time, and the maximum backpressure of the chromatographic system, to prevent prediction of unrealistic methods.

Provided that all necessary information is supplied, the program establishes the values of the retention parameters in both dimensions ($\ln k_0$ and S for ion-pair RPLC and $\ln k_0$ and n for IEC; see Sections 2.1 and 2.2), starting with an initial estimate, by utilizing MATLAB's fminsearch function for unconstrained nonlinear optimization. Initial guesses for the fminsearch function were 2 for both $\ln k_0$ and S in the case of RPLC, and 20 and 1 for $\ln k_0$ and n, respectively, in the event of IEC.

Table 1
Overview of optimization factors and their corresponding limits used for the optimization.

Factor	Minimum value	Maximum value	Number of steps	Increment
^1t_G	70	200	29	5
$^1t_{init}$	10	20	3	5
$^1c_{init}$	50	100	3	25
$^2\varphi_{init}$	0.05	0.2	4	0.05
$^2\varphi_{final}$	0.85	0.95	3	0.05

4.2. Validation

The system was programmed to predict one of the two experiments used to fit the retention parameters, with a ^1D gradient of 180 minutes, a ^2D gradient of 1.5 min and a modulation time of 2 minutes. Here, the system attempts to reproduce its input data and in this case there are no degrees of freedom so that good "prediction" performance is required. The program correctly described the retention times in both dimensions (Fig. 3), verifying that the program was functioning properly.

Next, the system was programmed to predict the chromatogram for a gradient of 360 minutes in the first dimension and 3 min in the second dimension. Here, the system is interpolating between the supplied data from the long and short gradient experiments, to validate the retention models. The result is shown in Fig. 4 with the prediction overlaid on the experimentally obtained chromatogram (Chromatogram without prediction overlaid provided in Supplementary materials Fig. S2). The prediction was found to be satisfactory with only slight deviations in the prediction of the retention times in the first dimension for a small number of the divalent anions (See Supplementary materials Table S2 for numeric data).

4.3. Optimization

In this study the optimization was limited to linear gradients in both dimensions. The program was configured to optimize a number of factors for each dimension, *viz.* the initial time before the gradient is set to start (t_{init}), the gradient time (t_G), and the initial and final organic modifier or buffer concentration of the gradient. For each of these factors, a range and a number of steps can be specified as valid outcome of the optimization. To limit the computation time required the user is advised to consider a limited number of parameters or a small number of steps at first, before zooming in on the most-important parameters, optimizing in smaller steps across a narrower range. In any case, the limits of each factor should be set taking into account the chromatographer's experience and insights. Table 1 describes the minimum and maximum values for each factor, as well as the number of steps between the limits that were tested.

Once the optimization factors and ranges are specified, the program will predict the chromatograms for all possible combinations. The present implementation of the program does not use peak-width data for the individual peaks from the scanning 2D chromatograms. Instead, it applies a generalized van-Deemter model in order to calculate the standard deviation of the peaks. For the first dimension we used $A = 2d_p$, $B = 3D_m$ and $C = (0.25\ {d_p}^2)/D_m$, and for the second dimension $A = 1.5d_p$, $B = 2D_m$ and $C = (0.05\ {d_p}^2)/D_m$. Here, d_p was in mm, $D_m = 10^{-3}$ mm^2 s^{-1} and u was calculated as the column length (in mm) divided by the dead time (in sec).

Several objectives were considered for the optimization. First, the quality of the separation was maximized. In order to measure the separation quality, the resolution between all peaks was calculated according to the metric for two-dimensional resolution described by Schure [18]. For every peak, the algorithm calculates the resolution with all other peaks. The resolution is then normalised to a value between 0 and 1 by using a Derringer desirability function [19–21]. For the case of resolution, the desirability function was

$$d\left(Rs_{i,j}\right) = \begin{cases} \dfrac{Rs_{i,j}}{1.5}\ if Rs_{i,j} < 1.5 \\ 1 if Rs_{i,j} \geq 1.5 \end{cases} \quad (8)$$

where $Rs_{i,j}$ is the resolution between peaks i and j, and $d\left(Rs_{i,j}\right)$ is the desirability function that varies between 0 (complete overlap) and 1 (no overlap, *i.e.* resolution 1.5 or higher). Note that the equation above has a ceiling. It considers that a resolution of 1.5 is satisfactory and that it is not worth it to put extra effort in separating peaks i and j further when such a resolution is achieved. If a lower limit is also desired, this can be implemented easily in the desirability function, simply setting $d\left(Rs_{i,j}\right)$ to 0 if the lower limit is reached [22]. Finally, the algorithm was set to take the product of all obtained resolution values to assess the overall separation quality, O_{Rs}

$$O_{Rs} = \prod_{i>j}^{m}\prod_{j=1}^{m} d\left(Rs_{i,j}\right) \quad (9)$$

where m is the total number of compounds considered.

The second objective considered was the analysis time. In this case, no desirability function was needed, and the time needed to elute the last eluted compound (in both dimensions) was considered to be the objective, O_{time}. This objective was obviously set to be minimized. Alternatively, other objectives can be considered. For example, the orthogonality of the separations (which was set to be maximized), O_{orth}. In this work, we followed the approach of Camenzuli and Schoenmakers [23] to calculate the orthogonality.

It is obvious that each combination of factors (Table 1) produces a set of objectives, namely, O_{Rs},O_{time} and O_{orth}. In order to handle this multi-objective optimization problem, a Pareto-optimization approach was applied (in this work, we considered only two objectives at the same time). For example, only O_{Rs} and O_{time} or O_{Rs} and O_{orth} were considered simultaneously. In short, Pareto optimization consists of plotting the two objectives considered for all possible combination of factors, and selecting the so-called Pareto-optimal conditions. A condition is considered Pareto-optimal if it is impossible to improve one of the objectives without worsening the other one(s). This results in a so-called Pareto front, which represent the performance limit within the specified constraints. Several of these Pareto fronts are depicted in Fig. 4 (panels a, b, c). The program also provides other options, as is shown in Fig. 5d, where one of the optimization factors (gradient time) is plotted against one of the objectives (resolution score, O_{orth}).

To test the prediction performance of the program for a gradient system with rather different conditions, a Pareto-optimal experiment was selected (depicted with an arrow in Fig. 4a). The experimental conditions corresponding to this point are as follows. The ^1D gradient ran from 0 to 100 mM in 70 min, after an initial hold time of 10 min. The ^2D gradient ran from 0.2 to 0.95 in 1.5 min (no initial hold time). The experimental LC × LC chromatogram and the prediction from the PIOTR program are shown in Fig. 6 (chromatogram without prediction provided in Supplementary materials Fig. S3). The performance was found to be particularly accurate in the RPLC dimension, whereas a number of significant deviations were observed in the IEC dimension (see Table 2).

The PIOTR program is intended for optimizing the separation selectivity, as opposed to the chromatographic efficiency. The former is determined largely by the two stationary phases, the temperature and – once these have been selected – the composition of the mobile phases in the two dimensions (as a function of time). We

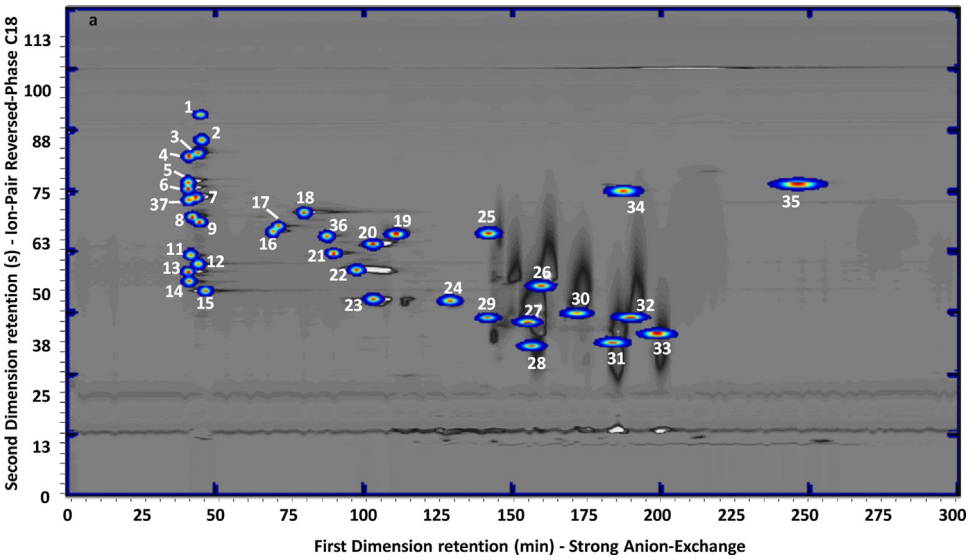

Fig. 3. Experimental LC × LC-UV chromatogram of the separation of a mixture of 54 dyes utilizing the fast gradients with the prediction of the PIOTR program as overlay.

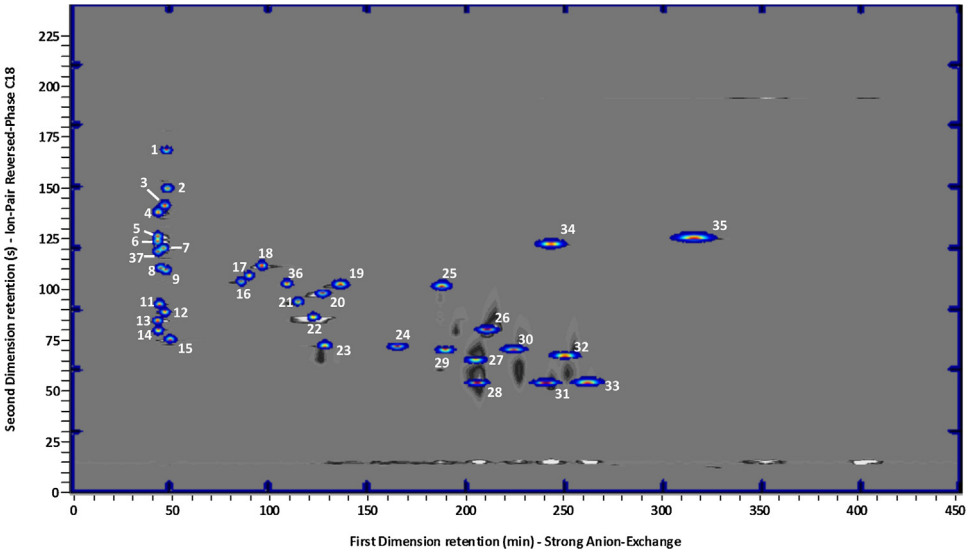

Fig. 4. The experimental LC × LC-UV chromatogram of the separation of a mixture of 54 dyes utilizing intermediate gradients with the prediction of the program as overlay. (see Supplementary materials Fig. S2 for the raw chromatogram without prediction overlay).

optimize an LC × LC set-up using the Pareto-optimization approach described previously [12]. During this stage due attention is paid to undersampling of the first-dimension signal and the effects on injection band broadening in the second dimension. We start using PIOTR on an LC × LC that has been optimized in terms of column dimensions, flow rates and modulation time.

Because in gradient-elution LC column length and flow rate and chromatographic selectivity are not strictly independent, it is feasible that optimized LC × LC separations can be improved further by repeating the cycle, *i.e.* re-optimizing the column dimensions and re-using PIOTR to fine tune the selectivity. In theory, the retention models previously obtained by PIOTR remain valid, if the stationary-phase chemistry remains unaltered.

4.4. Evaluation of the performance

As with the prediction based on interpolation in Fig. 4, the deviation in prediction accuracy occurred mainly for compounds eluting later in the first dimension, which are more strongly influenced by the gradient. Our equation for ion-exchange chromatography for compounds eluting after the gradient had never been published and, thus, has never been validated before. More experiments are required to rigorously validate it. However, we experienced poorly repeatable IEC separations during the course of the study, with retention times strongly shifting, likely due to inconsistencies in the column re-equilibration process (see Supplementary material Fig. S4 for 2D chromatograms). The error resulting from shifts in retention times is introduced in the fitted retention parameters. Hence, it propagates when the model is used to predict other conditions. The performance of the PIOTR program – or indeed any other program – is principally limited by the quality of the input data. Had the application employed RPLC × (IP)-RPLC rather than IEC × (IP)-RPLC, the performance would arguably have been better. Of course, an increase in the number of input experiments may also result in an improved prediction accuracy.

Another weak point in the ion-exchange dimension is the use of a linear gradient, whereas Eq. (5) shows the exponential charac-

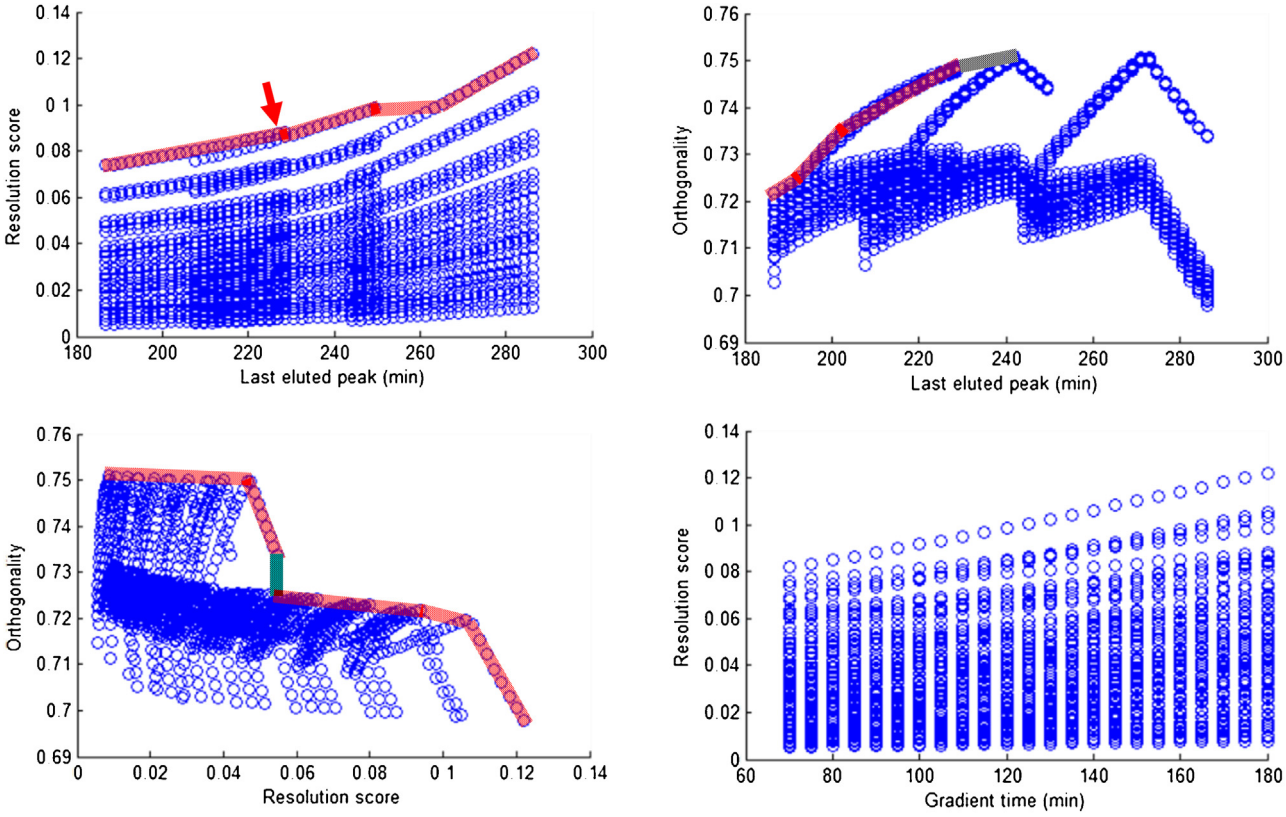

Fig. 5. Pareto-optimality plots using different factor combinations. a, resolution score (O_{Rs}) *vs.* the elution time of the last peak (O_{time}); b, orthogonality (O_{orth}) [23] *vs.* the elution time of the last peak (O_{time}); c, resolution score (O_{Rs}) *vs.* orthogonality (O_{orth}). Panel d depicts one of the factors (duration of the first-dimension gradient, ^1t_G) vs. resolution score (O_{Rs}). The red lines depict the Pareto-optimal fronts. The arrow depicts an example of a Pareto-optimal point.

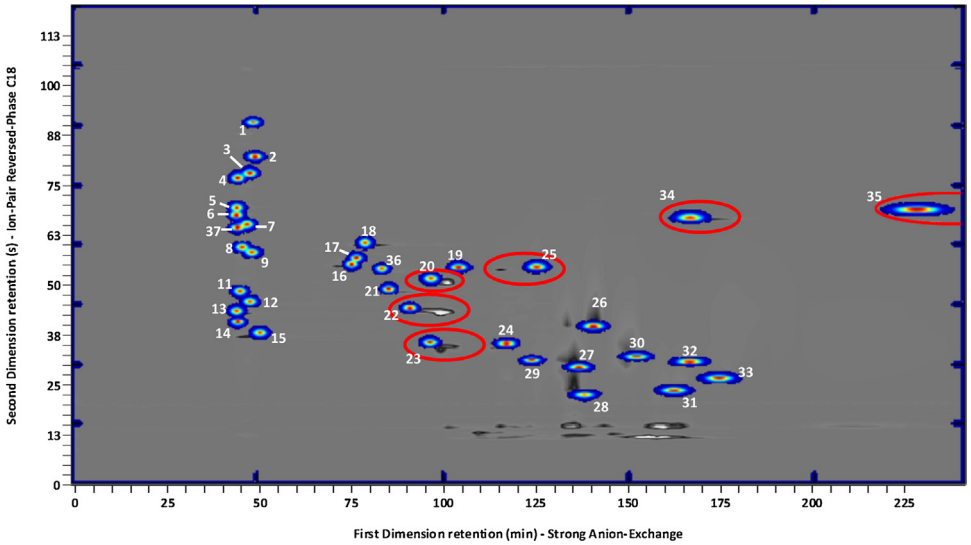

Fig. 6. Overlay of the experimental LC × LC-UV chromatogram of the separation of a mixture of 54 dyes utilizing Pareto-optimal gradients within the limits as stated in Section 4.3 and the retention times predicted by the PIOTR program. (see Supplementary materials Fig. S3 for the raw chromatogram without prediction overlay). The red circles highlight significant deviations between the predicted and observed retention time.

ter of retention in ion-exchange chromatography. An exponential gradient is thought to be more desirable in IEC.

The PIOTR program already has several strong points. The effects of many parameters on resolution or orthogonality can rapidly and rigorously be assessed. The Pareto-optimality approach in the program allows the selection of user-preferred optimal methods within specified limits. A very small number of scanning experiments (typically two) provide the user with a great deal of optimization data.

5. Conclusion

We have developed and demonstrated a computer program capable of predicting the retention behaviour for (ion-pair) reversed-phase and strong ion-exchange chromatography applied in LC × LC separation systems, based on just two scanning LC × LC experiments. Prediction of ion-pair reversed-phase behaviour was generally very accurate, whereas the prediction of ion-exchange retention can be improved. Overall, the PIOTR program can be

Table 2
Experimental verification of the optimum chromatogram predicted by the PIOTR program.

Peak ID[a]	First dimension			Second dimension		
	Experimental min	Predicted min	Difference min	Experimental min	Predicted min	Difference min
1	45.15	48.19	−3.05	1.47	1.51	−0.04
2	46.00	48.71	−2.71	1.35	1.36	−0.02
3	45.12	47.34	−2.22	1.30	1.29	0.01
4	44.13	44.16	−0.03	1.28	1.27	0.00
5	43.51	43.90	−0.39	1.15	1.15	0.00
6	43.03	43.78	−0.75	1.12	1.12	0.00
7	45.10	46.61	−1.51	1.08	1.08	0.00
8	44.23	45.32	−1.09	0.98	0.98	0.00
9	44.99	47.90	−2.91	0.96	0.96	0.00
11	44.52	44.75	−0.23	0.80	0.80	0.00
12	45.00	47.37	−2.37	0.76	0.76	0.00
13	43.73	43.85	−0.12	0.72	0.72	0.00
14	44.59	44.18	0.41	0.67	0.67	0.00
15	46.04	50.02	−3.98	0.62	0.63	0.00
16	70.94	75.54	−4.60	0.91	0.91	0.00
17	72.00	76.75	−4.75	0.94	0.94	0.00
18	79.07	78.93	0.14	1.00	1.00	0.00
19	101.55	103.14	−1.58	0.90	0.90	0.00
20	99.30	95.93	3.37	0.85	0.85	−0.01
21	88.48	84.87	3.61	0.81	0.81	0.00
22	96.90	90.37	6.54	0.72	0.73	0.00
23	99.90	95.66	4.24	0.58	0.59	0.00
24	112.00	115.34	−3.34	0.57	0.58	−0.01
25	114.45	123.04	−8.59	0.90	0.90	0.00
26	139.19	137.73	1.46	0.65	0.65	0.00
27	132.85	133.96	−1.11	0.51	0.48	0.03
28	133.46	135.42	−1.95	0.41	0.36	0.04
29	116.00	121.65	−5.65	0.49	0.51	−0.02
30	148.92	149.34	−0.42	0.58	0.53	0.05
31	158.00	160.52	−2.52	0.39	0.38	0.01
32	159.58	165.58	−6.00	0.51	0.50	0.00
33	162.00	175.46	−13.46	0.45	0.44	0.01
34	173.53	165.57	7.96	1.11	1.11	0.00
35	Not observed			Not observed		
36	87.00	83.15	3.85	0.89	0.89	0.00
37	44.76	44.05	0.71	1.07	1.07	0.00

[a] Compound 10 was excluded from optimization.

used to optimize LC × LC more rigorously, by taking into account multiple optimization parameters, and much more rapidly. Initial experience suggests that method development in LC × LC can be greatly accelerated, from (typically) several months to one week or less.

The PIOTR program can still be improved significantly. Firstly, predicting resolution hinges on our ability to accurately model the band broadening for all peaks. Incorporation of the peak width data of the two scanning experiments would thus be a large improvement. The widths of individual peaks may be taken into account in the PIOTR program. However, the effective resolution (fractional peak overlap) of peaks in LC × LC chromatogram should ideally also be considered. The fundamental dilemma that this brings about is that each sample will have its own optimum conditions, based on the relative intensities of the peaks.

Secondly, to avoid undersampling we deem it desirable to allow optimization of the modulation time in future improvements of the program. Furthermore, contemporary gradient systems often apply multiple steps in the gradient time program with different gradient slopes. For the program to be able to accommodate multiple steps in the gradient program, the currently used algorithm can be used and simply repeated, with each iteration representing a next gradient step.

Finally, some of the above mentioned potential improvements require or introduce additional factors for optimization and the computation time may become a limiting factor. Ultimately, alternative, more efficient optimization algorithms than the present brute-force approach should be explored.

Acknowledgements

The MANIAC project is funded by the Netherlands Organisation for Scientific Research (NWO) in the framework of the Programmatic Technology Area PTA-COAST3 of the Fund New Chemical Innovations (project C.2322.0291). Agilent Technologies is acknowledged for supporting this work, in particular Xiaoli Wang. Profs. José Ramon Torres Lapasió and M. Celia García Álvarez Coque from The University of Valencia (Spain) contributed as co-supervisors of two of the co-authors (SPT and COB). SPT would like to thank the Generalitat Valenciana for the postdoctoral grant APOSTD/2012/090.

Appendix A. Supplementary data

Supplementary data associated with this article can be found, in the online version, at http://dx.doi.org/10.1016/j.chroma.2016.04.061.

References

[1] P. Dugo, N. Fawzy, F. Cichello, F. Cacciola, P. Donato, L. Mondello, Stop-flow comprehensive two-dimensional liquid chromatography combined with mass spectrometric detection for phospholipid analysis, J. Chromatogr. A 1278 (2013) 46–53, http://dx.doi.org/10.1016/j.chroma.2012.12.042.
[2] R.J. Vonk, A.F.G. Gargano, E. Davydova, H.L. Dekker, S. Eeltink, L.J. de Koning, et al., Comprehensive Two-Dimensional Liquid Chromatography with Stationary-Phase-Assisted Modulation Coupled to High-Resolution Mass Spectrometry Applied to Proteome Analysis of Saccharomyces cerevisiae,

Anal. Chem. 87 (2015) 5387–5394, http://dx.doi.org/10.1021/acs.analchem.5b00708.
[3] A. D'Attoma, S. Heinisch, On-line comprehensive two dimensional separations of charged compounds using reversed-phase high performance liquid chromatography and hydrophilic interaction chromatography. Part II: Application to the separation of peptides, J. Chromatogr. A 1306 (2013) 27–36, http://dx.doi.org/10.1016/j.chroma.2013.07.048.
[4] K.M. Kalili, A. de Villiers, Systematic optimisation and evaluation of on-line, off-line and stop-flow comprehensive hydrophilic interaction chromatography × reversed phase liquid chromatographic analysis of procyanidins Part II: Application to cocoa procyanidins, J. Chromatogr. A 1289 (2013) 69–79, http://dx.doi.org/10.1016/j.chroma.2013.03.009.
[5] D.R. Stoll, D.C. Harmes, J. Danforth, E. Wagner, D. Guillarme, S. Fekete, et al., Direct Identification of Rituximab Main Isoforms and Subunit Analysis by Online Selective Comprehensive Two-Dimensional Liquid Chromatography–Mass Spectrometry, Anal. Chem. 87 (2015) 8307–8315, http://dx.doi.org/10.1021/acs.analchem.5b01578.
[6] E. Uliyanchenko, P.J.C.H. Cools, S. van der Wal, P.J. Schoenmakers, Comprehensive two-dimensional ultrahigh-pressure liquid chromatography for separations of polymers, Anal. Chem. 84 (2012) 7802–7809, http://dx.doi.org/10.1021/ac3011582.
[7] P. Dugo, M. del Mar Ramirez Fernandez, a. Cotroneo, G. Dugo, L. Mondello, Optimization of a Comprehensive Two-Dimensional Normal-Phase and Reversed-Phase Liquid Chromatography System, J. Chromatogr. Sci. 44 (2006) 561–565, http://dx.doi.org/10.1093/chromsci/44.9.561.
[8] H. Gu, Y. Huang, P.W. Carr, Peak capacity optimization in comprehensive two dimensional liquid chromatography: A practical approach, J. Chromatogr. A 1218 (2011) 64–73, http://dx.doi.org/10.1016/j.chroma.2010.10.096.
[9] H. Poppe, Some reflections on speed and efficiency of modern chromatographic methods, J. Chromatogr. A 778 (1997) 3–21, http://dx.doi.org/10.1016/S0021-9673(97)00376-2.
[10] K.M. Kalili, A. de Villiers, Systematic optimisation and evaluation of on-line, off-line and stop-flow comprehensive hydrophilic interaction chromatography × reversed phase liquid chromatographic analysis of procyanidins Part I: Theoretical considerations, J. Chromatogr. A 1289 (2013) 58–68, http://dx.doi.org/10.1016/j.chroma.2013.03.008.
[11] P. Cesla, T. Hájek, P. Jandera, Optimization of two-dimensional gradient liquid chromatography separations, J. Chromatogr. A 1216 (2009) 3443–3457, http://dx.doi.org/10.1016/j.chroma.2008.08.111.
[12] G. Vivó-Truyols, S. Van Der Wal, P.J. Schoenmakers, Comprehensive study on the optimization of online two-dimensional liquid chromatographic systems considering losses in theoretical peak capacity in first- and second-dimensions: A pareto-optimality approach, Anal. Chem. 82 (2010) 8525–8536, http://dx.doi.org/10.1021/ac101420f.
[13] P.J. Schoenmakers, H. a, H. Billiet, R. Tijssen, L. Degalan, Gradient Selection in Reversed-Phase Liquid-Chromatography, J. Chromatogr. 149 (1978) 519–537, http://dx.doi.org/10.1016/s0021-9673(00)81008-0.
[14] M.A. Quarry, R.L. Grob, L.R. Snyder, Prediction of precise isocratic retention data from two or more gradient elution runs. Analysis of some associated errors, Anal. Chem. 58 (1986) 907–917 http://www.scopus.com/inward/record.url?eid=2-s2.0-33845373548&partnerID=tZOtx3y1.
[15] G. Vivó-Truyols, J. Torres-Lapasió, M. Garcıía-Alvarez-Coque, Error analysis and performance of different retention models in the transference of data from/to isocratic/gradient elution, J. Chromatogr. A 1018 (2003) 169–181, http://dx.doi.org/10.1016/j.chroma.2003.08.044.
[16] B.W.J. Pirok, J. Knip, M.R. van Bommel, P.J. Schoenmakers, Characterization of synthetic dyes by comprehensive two-dimensional liquid chromatography combining ion-exchange chromatography and fast ion-pair reversed-phase chromatography, J. Chromatogr. A 1436 (2016) 141–146, http://dx.doi.org/10.1016/j.chroma.2016.01.070.
[17] P. Jandera, J. Churáček, Gradient elution in liquid chromatography, J. Chromatogr. A 91 (1974) 223–235, http://dx.doi.org/10.1016/S0021-9673(01)97902-6.
[18] M.R. Schure, Quantification of resolution for two-dimensional separations, J. Microcolumn Sep. 9 (1997) 169–176, http://dx.doi.org/10.1002/(SICI)1520-667X(1997)9:3<169:AID-MCS5>3.0.CO;2-#.
[19] K. Kamel, M.R. Hadjmohammadi, Application of Multilinear Gradient Elution for Optimization of Separation of Chlorophenols Using Derringer's Desirability Function, Chromatographia 67 (2007) 169–172, http://dx.doi.org/10.1365/s10337-007-0458-5.
[20] M. Hadjmohammadi, V. Sharifi, Simultaneous optimization of the resolution and analysis time of flavonoids in reverse phase liquid chromatography using Derringer's desirability function, J. Chromatogr. B Anal. Technol. Biomed. Life Sci. 880 (2012) 34–41, http://dx.doi.org/10.1016/j.jchromb.2011.11.012.
[21] B. Bourguignon, D.L. Massart, Simultaneous optimization of several chromatographic performance goals using Derringer's desirability function, J. Chromatogr. A 586 (1991) 11–20, http://dx.doi.org/10.1016/0021-9673(91)80019-D.
[22] A. Felinger, Data Analysis and Signal Processing in Chromatography, Elsevier Science Publishers B.V., 1998.
[23] M. Camenzuli, P.J. Schoenmakers, A new measure of orthogonality for multi-dimensional chromatography, Anal. Chim. Acta 838 (2014) 93–101, http://dx.doi.org/10.1016/j.aca.2014.05.048.